Available online at www.sciencedirect.com
SCIENCE DIRECT
Energy and Buildings 38 (2006) 1022–1031
ENERGY and BUILDINGS
www.elsevier.com/locate/enbuild

Wall heat loss from intermittently conditioned spaces—The dynamic influence of structural and operational parameters

P.T. Tsilingiris

Department of Energy Engineering, Technological Education Institution (TEI) of Athens, A. Spyridonos Str. GR 122 10, Egaleo, Athens, Greece

Received 22 June 2005; received in revised form 7 November 2005; accepted 17 November 2005

Abstract

The intermittent daily operation of the HVAC equipment is currently a method usually adopted for reasons of proper building energy management in geographical regions with temperate climatic conditions. Under these conditions, the influence of the building envelope and the specific operational schedule of the mechanical equipment under the effect of time-varying ambient temperature and incident solar radiation is responsible for the development of complex transient heat transfer phenomena, which leads to continuous heat exchange with the environment. The heat exchange through the building envelope, which determines its energy efficiency, is strongly influenced by several parameters along with the thermal characteristics of the building elements like the wall thermal resistance and heat capacity as well as the thermal time constant and operational conditions of mechanical equipment. In the present investigation, an analysis is developed for the evaluation of the daily quasi steady-state energy losses from composite walls under the effect of time-varying meteorological driving forces, when heating at the room side is intermittent.

The effect of various significant design and system operational parameters like wall heat capacity, thermal time constant and the insulation layer configuration, daily heating cycle duration and phase, as well as room heat capacity and net heating power input are investigated on the quasi steady-state energy loss and daily room temperature swing under typical winter conditions.

Keywords: Transient wall performance; Intermittent heating load; Heat capacity distribution; Wall thermal time constant; Building heat transfer

1. Introduction

The remarkable current interest in the thermal performance of buildings is attributed to the substantial energy consumption and associated environmental impacts for maintaining indoor comfort conditions. Energy is a significant cost component during the operational life of buildings, in the current economic environment of the ever rising costs of fossil fuels. A substantial amount of research work has been carried out during the last two decades in the area of the dynamic thermal behavior of walls and on their impact to building energy use, since they are the most important components affecting seriously the energy efficiency. Previous extensive research on wall heat transfer, has mostly been based on equivalent electrical network theory and numerical methods [1–5], although their effect was also investigated to allow the determination of the dynamic thermal parameters of the whole building [6,7].

The wall heat capacity affects its transient thermal behavior considerably, leads to slower response to the imposed meteorological driving forces and improves the long-term energy efficiency, so as thermal resistance as derived from simple steady-state considerations, does not reflect a reliable energy conservation indicator for walls. For this reason new criteria like thermal mass benefit are put forward for consideration, aiming possibly at the performance evaluation and wall rating [8]. The use of a massive building envelope leads to reduction and phasing out of peak loads, something which can easily be quantified by the definition of the wall damping-out efficiency factors which were calculated for a broad range of typical walls by Tsilingiris [9]. It has also been suggested that the transient response of a particular wall under the effect of a step temperature change may reveal a new wall property, the wall thermal time constant, which reflects the spatial distribution of heat capacity and has strongly directional characteristics [10]. The presence of thermal insulation layers may considerably affect the spatial distribution of heat capacity in composite walls, owing to their low density. Therefore, proper design of thermal insulation may significantly

E-mail address: ptsiling@teiath.gr.

0378-7788/$ – see front matter © 2006 Elsevier B.V. All rights reserved.
doi:10.1016/j.enbuild.2005.11.012

Nomenclature

A	area (m^2)
c	specific heat capacity (J/kg K)
HCA	per unit surface area heat capacity (J/m^2 K)
h	convective heat transfer coefficient (W/m^2 K)
I	incident solar radiation (W/m^2)
K	numerical constant
k	thermal conductivity (W/mK)
L	wall thickness (m)
m	mass (kg)
n	number of sublayer sections Δx
P	pressure (Pa)
p	number of time increments Δt
Q	heat rate (W)
q	heat flux rate (W/m^2)
R	Gas constant (J/kg K)
t	time (s)
T	temperature (°C)
TC	time constant (s)
U	overall heat transfer coefficient, U value (W/m^2 K)
V	volume (m^3)
x	space coordinate (m)

Greek letters

α	total hemispherical absorptivity
Δ	difference
δ	layer thickness (m)
λ	dimensionless parameter
ρ	density (kg/m^3)
φ	phase angle (degree)

Subscripts

a	air
c	concrete
co	convective, room side
c∞	convective, ambient side
d	domain
eff	effective
F	forward
f	floor
i	thermal insulation, node number
in	input
m	interior mass
N	number of days
n	net
o	room
pa	pressure, air
r∞	radiative, ambient side
ro	radiative, room side
R	reverse
w	wall
∞	ambient

improve the energy efficiency of buildings as in the situations of continuously conditioned spaces, when it is usually installed at the ambient side of external walls. Under these conditions, the distribution of heat capacity close to room space contributes strongly to the effective suppression of room temperature swings, although very often in practice the choice of thermal insulation location is rather more usually based on convenience of construction and cost.

The effects of heat capacity and insulation location on wall structure factors was recently investigated by Kossecka and Kosny [11], who also illustrated their influence on a continuously used building performance, employing a whole building dynamic simulation.

The effect of wall heat capacity and its spatial distribution on the developed time depended heat flux, caused by time-varying meteorological driving functions was recently investigated under the assumption of a fixed room temperature [12]. According to results from extensive comparative computer simulations between walls of equal thermal resistance though of a broadly varying heat capacity, it was derived that the spatial distribution of heat capacity which is determined by the wall thermal time constant, affects remarkably the time depended heat flux during the development of the transient, even though there is absolutely no effect of heat capacity and its spatial distribution on the developed quasi steady-state wall heat flux.

However, the operation of the HVAC equipment in the majority of buildings, at least as far as in tempered geographical regions of the world is concerned, is intermittent owing to various reasons, ranging from proper energy management and administration to the specific application of the building. This is particularly valid for the central heating installations, which are currently considered to be standard systems for the majority of domestic, public and commercial buildings. At the same time, the importance of proper thermal insulation design in existing and new buildings steadily grows in the environment of an erratic energy supply and a growing energy cost. The heating cycle for certain groups of social, commercial as well as public buildings is practically limited to only a few hours daily, while energy conservation strategies for residential buildings tend steadily to impose short daily heating cycles, specifically for a period of the maximum expected occupancy, even in geographical areas with a considerable number of degree-days of heating.

Although explicit reference in the analysis is made to walls as the main vertical structural elements of the building envelope, the derived results can also almost equally be applied to horizontal structural elements like roofs and ceilings. This is attributed to the fact that they act much like walls, with the exception of the more significant influence of the external surface radiating properties and of the importance of the specific horizontal orientation on convective heat transfer processes.

2. Theoretical analysis

Conduction heat transfer in building envelope elements may be very complex owing to the effect of structural irregularities metal studs and thermal bridges, causing strongly three-

dimensional effects. Ignoring such effects and assuming large lateral dimensions to minimize edge effects, the conduction heat transfer at a direction perpendicular to building element surface is predicted by the following one-dimensional heat conduction equation:

$$\frac{\partial}{\partial x}\left[k \cdot \frac{\partial T(x,t)}{\partial x}\right] = \rho \cdot c \cdot \frac{\partial T(x,t)}{\partial t} \tag{1}$$

It is also assumed that the ambient side of the wall of thickness L is subjected to the diurnal time-varying effect of incident solar radiation and ambient temperature $I(t)$ and $T_\infty(t)$, respectively, and that the coordinate system is located at its ambient side. Under these conditions, the heat flux at the ambient wall side is derived by the following expression:

$$q(0,t) = \alpha \cdot I(t) + (h_{c\infty} + h_{r\infty}) \cdot [T(0,t) - T_\infty(t)] \tag{2}$$

where α, $h_{c\infty}$ and $h_{r\infty}$ are the total ambient wall side hemispherical absorptivity, convective and radiative heat transfer coefficients, respectively. This quantity is calculated from Fourier's law:

$$q(0,t) = -k \cdot \frac{\partial T(0,t)}{\partial x} \tag{3}$$

The corresponding heat flux at the room side is:

$$q(L,t) = (h_{co} + h_{ro}) \cdot [T_o(t) - T(L,t)] \tag{4}$$

where h_{ri}, h_{ro} are the convective and radiative heat transfer coefficients for the room side and the heat flux at the room side calculated by Fourier's law:

$$q(L,t) = -k \cdot \frac{\partial T(L,t)}{\partial x} \tag{5}$$

The time depended value of the room air temperature as appeared at the right hand side of Eq. (4), is derived by the following room heat balance equation:

$$Q_n(t) - Q(L,t) = (m \cdot c)_{eff} \cdot \frac{\partial T_o(t)}{\partial t} \tag{6}$$

where $(m{\cdot}c)_{eff}$ is the effective heat capacity of the room node and Q_n is the net heating power at the room side. Its physical significance represents the sum of the heat input power Q_{in} of the room side terminal heater and the ventilation–infiltration heat loss Q_a:

$$Q_n(t) = Q_{in}(t) - Q_a(t) \tag{7}$$

and $Q(L, t)$ is the overall heat transfer from the room side as derived from (4):

$$Q(L,t) = (h_{co} + h_{ro}) \cdot A_w \cdot [T_o(t) - T(L,t)] \tag{8}$$

where A_w is the wall surface area.

The structural elements of the building envelope represent usually walls floors and ceilings enclosing the whole internal mass of the structure. This is the sum of interior and room air mass and therefore a first order approach for the calculation of the room side temperature node is to assume that internal mass is uniformly distributed over the surface area of the building envelope into a lumped value.

However, this simplified assumption is not always valid, especially when large internal masses are involved like partitions, other than simple lightweight movable panels. Under these conditions, since the distributed mass of interior space is usually weakly coupled to the room air through natural convection and radiation conductances, its temperature may lag considerably the room temperature node. This behavior is expected to be even more pronounced in the presence of heavy brick partitions or even heavier concrete or concrete-water walls, usually employed in passive solar design. The use of such building elements may lead to considerable time lag, complex heat exchange between the distributed mass of interior space and violation of the lumped parameter model assumption.

From Eqs. (6) and (8) it is derived that:

$$q_n(t) - (h_{co} + h_{ro}) \cdot \left(\frac{A_w}{A_f}\right)[T_o(t) - T(L,t)] = \frac{(m \cdot c)_{eff}}{A_f} \cdot \frac{\partial T_o(t)}{\partial t} \tag{9}$$

with $q_n(t)$ the per unit floor area net power input at the room side. In this expression, the effective heat capacity, which determines the transient thermal response of the lumped room temperature node, may considerably vary as the presence of internal mass is mostly unpredictable.

Therefore, it would be possible at this stage, to fix the room heat capacity to a value corresponding only to room air mass, neglecting the effect of interior mass. This simplifying assumption allows the investigation of the fundamental behavior of the present basic model, without affecting the physical significance of the derived results. The sensitivity of the derived results from the effect of heat capacity of the room temperature node can further be investigated by parametric analyses, allowing a broad range variation of this quantity.

Assuming for simplicity negligible radiative heat exchange, the previous expression becomes:

$$q_n(t) - \lambda \cdot h_{co} \cdot [T_o(t) - T(L,t)] = \frac{P_a}{R_a} \cdot c_{pa} \cdot \left(\frac{V}{A_f}\right) \cdot \frac{1}{T_o(t)} \cdot \frac{\partial T_o(t)}{\partial t} \tag{10}$$

with P_a, R_a are the normal atmospheric pressure and gas constant for air, respectively, and (V/A_f) the ratio of the enclosed air volume per unit floor area at the room side.

The dimensionless parameter λ, defined as:

$$\lambda = \frac{A_w}{A_f} \tag{11}$$

may vary considerably, depending on the proportion of room wall to floor area. This parameter being based on the specific design considerations is directly related to the geometry of internal space and lacks any other physical significance.

3. The description of wall samples

Three groups of composite, thermally insulated walls were selected. For simplicity, each group is composed from a certain specific number of fixed thickness concrete layers of $c_c = 880$ J/kg K, $\rho_c = 2300$ kg/m^3 and $k_c = 1.40$ W/m K and a single thermal insulation layer of the same thickness and $c_i = 840$ J/kg K, $\rho_i = 40$ kg/m^3 and $k_i = 0.041$ W/m K, respectively. The so developed number of composite walls in each group depends on the specific arrangement of the successive thermal insulation (shaded layer) and concrete layers (clear layers), as shown in Fig. 1, and the composite wall thickness L, which is a fixed multiple of the layer thickness δ. Assuming in all cases fixed film resistances corresponding to $h_{co} = 8$ W/m^2 K and $h_{c\infty} = 20$ W/m^2 K for the room and ambient side, respectively, all the walls of each group are of uniform thermal resistance. For a layer thickness of $\delta = 6$ cm, the composite wall group A with a width of $L = 0.18$ m, develops three different walls, the walls A1, A2 and A3 corresponding to the thermal insulation layer location at the room, the mid-plane and the ambient side of the wall, respectively. The second group of composite walls B with a width of $L = 0.24$ m, develops the four different walls B1, B2, B3 and B4, while the third group C, with a width of $L = 0.30$ m develops the following five walls C1, C2, C3, C4 and C5, as shown in Fig. 1, with the walls A1, B1 and C1 corresponding to the thermal insulation layer placed at the room side. The so developed composite walls of each group are of a uniform U value and per unit wall surface area heat capacity, which are defined by the following expressions:

$$U = \left[\frac{1}{h_{co}} + \delta \cdot \sum_{i=1}^{n} \frac{1}{k_i} + \frac{1}{h_{c\infty}}\right]^{-1} \tag{12}$$

$$\text{HCA} = \delta \cdot \sum_{i=1}^{n} \rho_i \cdot c_i \tag{13}$$

where n is the number of layers in each group of thickness δ. These uniform quantities for the three wall groups A, B and C are equal to $U = 0.580$, 0.566, 0.552 W/m^2 K and

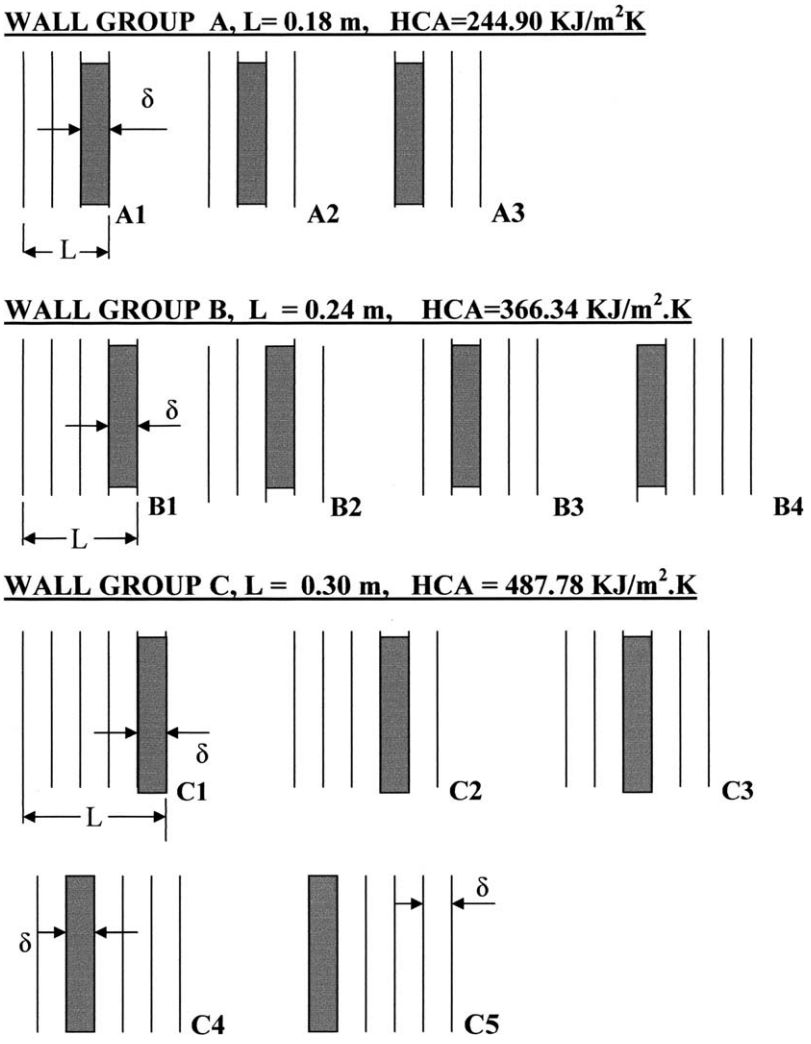

Fig. 1. The description of the three groups A, B and C of wall samples.

HCA = 244.90, 366.34 and 487.78 kJ/m^2 K, respectively. However, the distribution of heat capacity at a direction perpendicular to the wall plane for these walls is broadly different. The spatial distribution of heat capacity can be described by a recently introduced physical quantity, the wall thermal time constant. This quantity, which was proposed to quantify how rapidly an isothermal wall at thermal equilibrium responds to a properly defined step temperature change of air imposed at a particular wall side, was found to have strongly directional characteristics [10]. These are associated with the boundary conditions and the spatial distribution of heat capacity, which is generally different in respect of the specific wall side, something which leads to the definition of the forward $(TC)_F$ and reverse time constants $(TC)_R$, which are not usually equal.

Both time constants can easily be calculated, by the numerical solution of Eq. (1) for an initially isothermal wall under the appropriate boundary conditions, referring to specific temperatures and convective heat transfer coefficients at the fixed temperature and the opposite wall side, where the temperature step is applied. Assuming deliberately that forward time constant is defined when the temperature step is applied at the room side, the reverse time constant is calculated when an identical temperature step is applied at the opposite wall side. Its numerical value is determined as in the usual way in physics, by evaluating the time required for a time depended quantity, namely the heat flux, to become the e^{-1} fraction of its initial value. Assuming identical convective heat transfer coefficients at both wall sides, the calculated numerical value of the ratio $[(TC)_F/(TC)_R]$ is indicative of the spatial distribution of heat capacity in a composite wall. Presence of a large heat capacity closely to the room side leads to values of $[(TC)_F/(TC)_R] > 1$, otherwise $[(TC)_F/(TC)_R] < 1$, while a symmetrical distribution of heat capacity, respectively, to the wall mid-plane leads to $[(TC)_F/(TC)_R] = 1$.

The thermal time constants for all the walls of the three groups A, B and C were calculated assuming an initially isothermal wall at 5 °C under the effect of a step air temperature change of 20 °C at the one side, when the opposite is fixed at 5 °C, with the $h_{co} = 8$ W/m^2 K and $h_{c\infty} = 20$ W/m^2 K and the results are shown in Table 1. According to the derived results, it can be seen that the values of forward and reverse time constants are not identical for the symmetrical walls A2 and C3, owing to the considerable difference between the convective heat transfer coefficients. It can also be seen clearly that the minimum values of the forward and reverse wall thermal time constants correspond to the walls with the thermal insulation layer placed at the room or the ambient wall side, respectively.

4. The development of numerical model

The solution of the one-dimensional conduction heat transfer Eq. (1) with the appropriate boundary conditions (2)–(5) was derived numerically using the finite difference method. Towards this aim the width of the wall L was subdivided into n isothermal sublayer sections of a thickness Δx, so as $L = n \cdot \Delta x$. The density, heat capacity and thermal conductivity of these sublayers were assumed to be uniform. Each sublayer of uniform temperature corresponds to a node of a thermal network, which is terminated at the boundary nodes corresponding to the ambient and room air temperatures. The entire time domain of integration t_d is also subdivided into a number p of time increments Δt, so as $t_d = p \cdot \Delta t$. The expressions (1)–(5) were translated into a set of simultaneous algebraic equations, corresponding to each inner and boundary node of the thermal network, using the always inherently stable, implicit Laasonen or alternatively Crank–Nickolson finite difference approximation [13,14], as also discussed in greater detail in previous publications [5,9].

The accuracy of numerical solution improves as the nodal grid becomes fine, corresponding to a large number of sublayer sections Δx, and the time step increment Δt, respectively, decrease. Thus, the selection of the optimum number of sublayer sections and time increment, which determines the number of the thermal network nodes and the overall number of integration time steps, respectively, is a trade-off between computer CPU time and desired accuracy level of calculations. This selection, which was based on extensive numerical experiments, corresponds usually to a sublayer thickness of 1 cm and a time step between 60 and 300 s, and the results were

Table 1
The calculated time constants for the three groups of walls A, B and C

Wall group	Wall type	Forward time constant $(TC)_F$ (h)	Reverse time constant $(TC)_R$ (h)
"A", HCA = 244.90 kJ/m^2 K;	A1	0.169	3.370
$U = 0.580$ W/m^2 K	A2	4.110	1.934
	A3	7.916	0.163
"B", HCA = 366.34 kJ/m^2 K;	B1	0.180	4.21
$U = 0.566$ W/m^2 K	B2	4.180	3.385
	B3	7.950	1.937
	B4	11.10	0.164
"C", HCA = 487.78 kJ/m^2 K;	C1	0.184	4.380
$U = 0.552$ W/m^2 K	C2	4.210	4.136
	C3	7.970	3.396
	C4	11.15	1.194
	C5	13.07	0.165

successfully evaluated against analytical solutions from the theory [9].

The modeling of the time-varying meteorological driving forces which are represented by the instantaneous values of incident solar radiation and ambient temperature in Eq. (2), was based on existing long-term, statistically treated sample of some 25 years of solar radiation measurements from the National Observatory of Athens for the period 1961–1980. These measurements were integrated over all hours of the day to derive average daily values of incident solar radiation in a horizontal plane. The derived long-term statistically treated daily average data are employed to derive hourly values of incident solar radiation at a vertical south-faced plane, according to the well established procedures [15], as also extensively discussed in previous publications [16,17]. The necessary instantaneous values of incident solar radiation at the vertical south-faced wall in W/m^2 for winter simulations which correspond to a typical winter day, the 20th of January, were derived by the following simple polynomial fit expression of the derived hourly data, valid for the sunshine hours of the day:

$$I(t) = K_1 + K_2 \cdot t + K_3 \cdot t^2 + K_4 \cdot t^3 + K_5 \cdot t^4 \quad (14)$$

where t is the time in hours from the midnight and K_i, $i = 1$–5, numerical constants with typical values of $K_1 = 1463.74$, $K_2 = -897.912$, $K_3 = 157.295$, $K_4 = -9.99013$, $K_5 = 0.208128$, corresponding to this specific day of the year.

The calculation of the instantaneous values of the employed ambient temperature is based on existing long-term daily range, maximum and average temperatures for each day of the year for Athens, which were derived by statistical treatment of long-term temperature measurements during the period 1950–1975. After fitting by harmonic functions, these data were employed for the calculation of the ambient temperature throughout the day, according to the model proposed by ASHRAE [18]. For the purpose of the present investigation, the derived hourly data corresponding to the typical winter day of the 20th of January were fitted with a good accuracy by the following simple, single term harmonic function:

$$T_\infty(t) = \bar{T} + T_m \cos\left(\frac{2\pi}{24} \cdot t - \varphi\right) \quad (15)$$

with typical average and amplitude values $\bar{T} = 8.62\,^\circ$C and $T_m = 3.68\,^\circ$C, respectively, and a phase angle of $\varphi = 225^\circ$.

Having realized from previous investigations that the time domain of 5 sequential days of simulations for certain walls of a large heat capacity is rather short [12], it was decided to extend the time domain of the present investigations to a period of 8 days or 192 h, corresponding to 8 successive days, during which quasi steady-state solutions are developed after all transients have died away. It is assumed that the heating is intermittent and lasts during a desired specific daily period of time, starting at a particular hour of the day. For the purpose of the present investigations, the starting time of the daily heating cycle was selected at midnight, 6 h and 12 h from midnight and the time duration of the intermittent heating cycle simulations was taken to be 4, 8 and 12 h daily, corresponding to a (T_L/T_D) ratio of 4/24, 8/24 and 12/24, respectively, for all the walls of the three groups. Since the parameter λ has only a geometrical significance and it represents a multiplication constant to the convective heat transfer coefficient h_{co} in (10) which was deliberately assumed to be equal to $h_{co} = 8$ W/m^2 K, its numerical value was decided to be taken equal to unity for the subsequent calculations, without affecting considerably either the accuracy or the physical significance of the derived results. The per unit floor area net power input was also taken equal to $q_n = 37$ W/m^2, while a value of 0.7 m was selected for the ratio (V/A_f) for the calculations. Subsequent sensitivity analysis was also carried out, to investigate the effects of variation of these parameters on the derived results, with twice as high values of $q_n = 75$ W/m^2 and appreciably higher values of (V/A_f) = 3.0 and 6.0 m.

5. Results and discussion

Typical results corresponding to 8 simulation days are shown in Fig. 2 for the walls of the group C, with HCA = 487.78 kJ/m^2 K for a daily heating period of 8 h, starting at 6 h from midnight with an initial room temperature of 15 °C for $q_n = 37$ W/m^2 and (V/A_f) = 0.7 m. In the same plot, the total incident solar radiation at a south-faced wall of a total hemispheric absorptivity of $\alpha = 0.5$ and the ambient temperature are shown in solid and dotted lines, respectively. The heavy solid line represents the time-varying room node temperature for the wall C1 of $(TC)_F = 0.184$ h, corresponding to the thermal insulation layer placed directly at the room side. As derived from Fig. 2, this temperature falls rapidly during the first few hours with the heater being off, owing to the convective

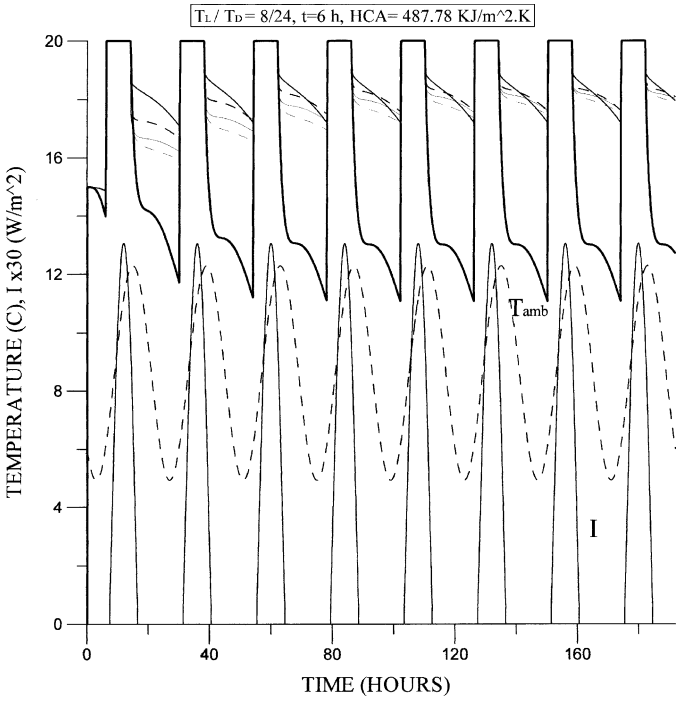

Fig. 2. The prediction of the time dependence of the room temperature node for the walls of group C, C1–C5. Lower thin solid and broken lines correspond to the incident solar radiation (I) and ambient temperature (T_{amb}), respectively.

coupling between wall and room air. When the heating cycle begins at 6 h, the room heater at full capacity goes on and causes a rapid increase of room temperature node up to the desired thermostat setting level of 20 °C. Then, its heating power capacity is appropriately controlled to maintain a fixed room node temperature equal to 20 °C, until the termination of the daily heating cycle of 8 h. Immediately after this, when the terminal heater goes off, the room node temperature decreases rapidly up to the minimum temperature before the next day heating cycle begins. Under these conditions the system develops asymptotically quasi steady-state behavior and leads to the development of quasi steady-state solutions, corresponding to an appreciable range of daily room node temperature swing higher than 12 °C. This practically occurs within a period of about 80 h, owing to lack of large heat capacity layers close to the room side for the wall C1. As soon as the thermal insulation layer moves towards ambient side, redistribution of mass leads to a substantial increase of heat capacity close to room side, something which causes a subsequent increase of the forward time constant, although the wall thermal resistance remains unchanged. This has a remarkable effect on the wall dynamic behavior, as shown by the succession of the thin solid and broken lines in Fig. 2, corresponding to the walls C2 to C5, showing the developed room node temperature during the daily period when the heater is off. Increase of heat capacity close to the room side corresponds to a forward time constant increase from 4.210 to 13.07 h for the walls C2 to C5 respectively and leads to a substantial reduction of the room node daily temperature swing. This swing becomes minimum, almost 3 °C for the wall C5, with a substantial corresponding increase of transient, which allows the development of quasi steady-state solutions not earlier than 150 h.

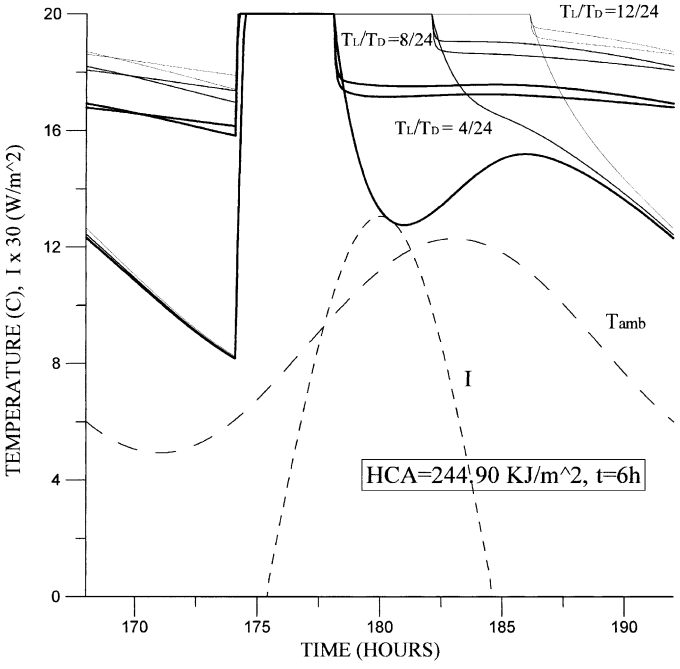

Fig. 3. The effect of the daily heating cycle duration and wall thermal time constant, on the developed quasi steady-state room node temperature. In the same plot, the incident solar radiation at a south-faced wall and the ambient temperature are also shown in broken lines.

The effect of the heating cycle duration on the quasi steady-state room node temperature corresponding to $N = 8$, for all the walls of group A of HCA = 244.90 kJ/m^2 K is shown in Fig. 3, for $q_n = 37$ W/m^2 and $(V/A_f) = 0.7$ m, when the heating cycle begins at $t = 6$ h. Except for the incident solar radiation and ambient temperature, there are also plotted three groups of curves, corresponding to a daily heating cycle duration of 4, 8 and 12 h, consisting of three specific curves each, drawn with lines of a uniform thickness. The lower curve in each group corresponds to the wall A1, the mid curve to A2 while the upper curve to A3. It can clearly be seen that for the first group of curves plotted with the heavier lines, the wall A1 with the minimum forward time constant leads to the maximum daily room node temperature swing of about 12 °C, with a minimum occurring just before the terminal heater goes on. After the termination of the heating cycle, there is a rapid decrease of the room temperature node, which shortly after midday increases again to a maximum level of almost 16 °C at about 5:30 p.m., owing to the delaying effect of the wall thermal inertia on the peak value of meteorological driving forces. The wall A2 (mid curve) leads to a substantial reduction of the daily temperature swing to almost 4 °C, while the wall A3 further reduces the temperature swing, although at a much lower level. The increase of the daily heating cycle duration to 8 and 12 h, as shown by the next two groups of thin solid lines, although it leads to a comparable daily temperature swing for the wall A1, contributes significantly to the further reduction of the temperature swing level of about 3 and 2 °C for the subsequent walls A2 and A3, respectively.

The time depended heat flux at the room side of the wall $q(L, t)$ during the whole period of simulation can be calculated from the expression (4). The amount of energy lost from the room side surface of the wall during the N day of simulation is calculated by the following expression:

$$Q(n, L) = \int_{N-1}^{N} h_{co} \cdot [T(L, t) - T_o(t)]\, dt \tag{16}$$

which for $N = 8$ represents in all cases a very important quasi steady-state quantity. This is the net amount of energy which crosses the wall boundary during the specific period of time and depends on the dynamic interaction of a large number of design, operational and environmental parameters, like the thermophysical properties of the specific composite wall materials, geometric design and configuration of layers, the starting time and daily duration of the heating cycle, as well as on the meteorological driving forces. These parameters affect considerably the daily amount of heat stored and determine the effect of interrelated complex dynamic processes to the thermal behavior and energy performance of the specific wall.

Typical quasi steady-state simulation results for $N = 8$ and all the walls of the group "B" with HCA = 366.34 kJ/m^2 K, corresponding to higher values of $q_n = 75$ W/m^2 and $(V/A_f) = 3$ m, are shown in Fig. 4 for a heating cycle of 8 h starting at 6 h

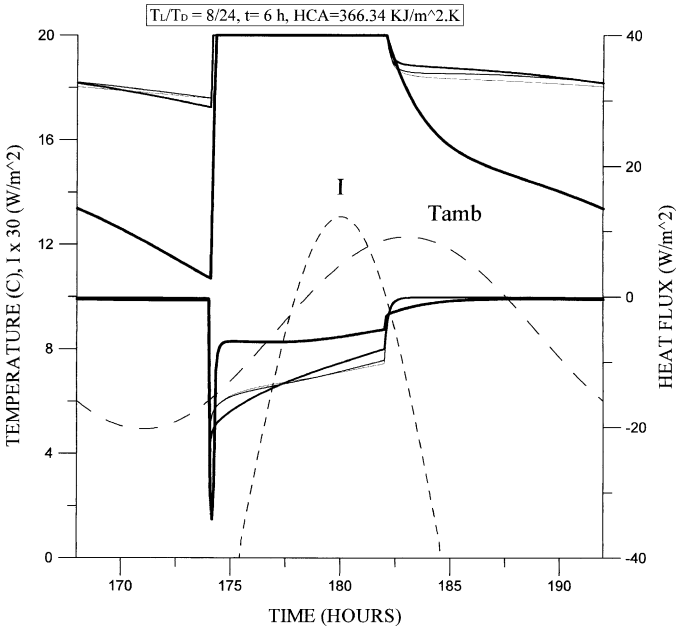

Fig. 4. The effect of the space distribution of heat capacity on the quasi steady-state room node temperature and heat flux for the walls of group B. The incident solar radiation at a south-faced wall and the ambient temperature are also shown in broken lines.

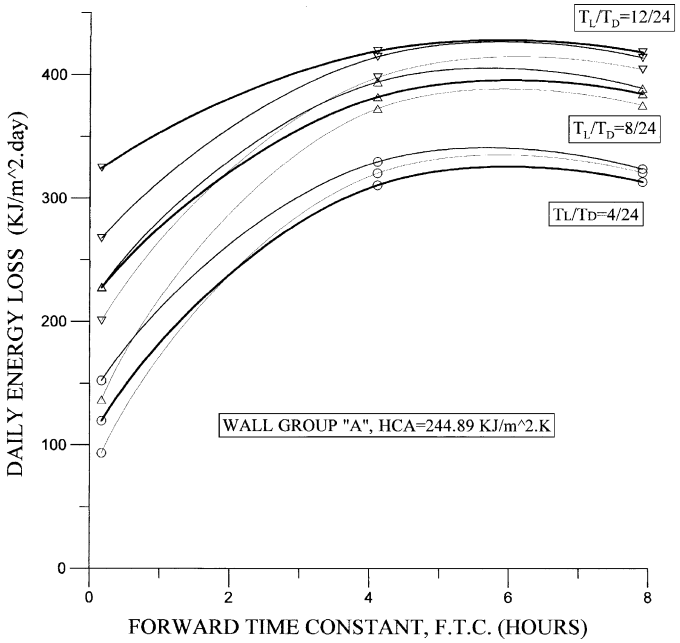

Fig. 5. The calculated quasi steady-state energy lost daily for the walls of group A as a function of the forward wall time constant.

after midnight, in which the room node temperatures and corresponding heat fluxes are plotted. In the same figure, the instantaneous values of incident solar radiation and ambient temperature are also shown by the dotted and broken lines, respectively.

As shown by the top heavy solid line corresponding to the wall B1, a rapid increase of room temperature node up to the thermostat set level, which occurs at $t = 6$ h owing to the operation of the terminal heater, is followed by a slow corresponding decrease, leading to a daily temperature swing of almost 10 °C. As shown by the corresponding lower heavy solid line for the same wall, a short duration transient heat flux spike of almost 35 W/m^2 is developed when the terminal heater goes on, suggesting large instantaneous temperature differences between wall and room air. This is followed by a slowly decreasing heat flux until the termination of the heating cycle. After this, the heat flux gradually diminishes to a very low negative value. The total surface area between heavy and zero heat flux lines, represents the daily quasi steady-state amount of energy crossing the wall boundary, which corresponds to the numerical value of integral (16), for $N = 8$.

The corresponding behavior of the subsequent higher forward time constant walls B2, B3 and B4 of the same group is shown by the thinner solid lines in the same plot. A remarkably lower, almost 3 °C, daily temperature swing is developed for the wall B2, while a slight subsequent reduction of the same quantity occurs for walls B3 and B4. At the same time as derived from the corresponding heat flux lines below, although instantaneous heat flux spikes of comparable maximum value are developed immediately after the heater goes on, their time depended values during the heating cycle are higher, owing to the effect of increased heat storage at the wall layers close to the room space.

The quasi steady-state energy crossing the wall boundary at the room side as calculated from (16) for $N = 8$, represents the amount of energy lost daily. This quantity is plotted by appropriate fitting of the derived data, as a function of the forward time constant and $q_n = 37$ W/m^2, $(V/A_f) = 0.7$ m, for all the walls of the groups A, B and C in the Figs. 5–7, respectively.

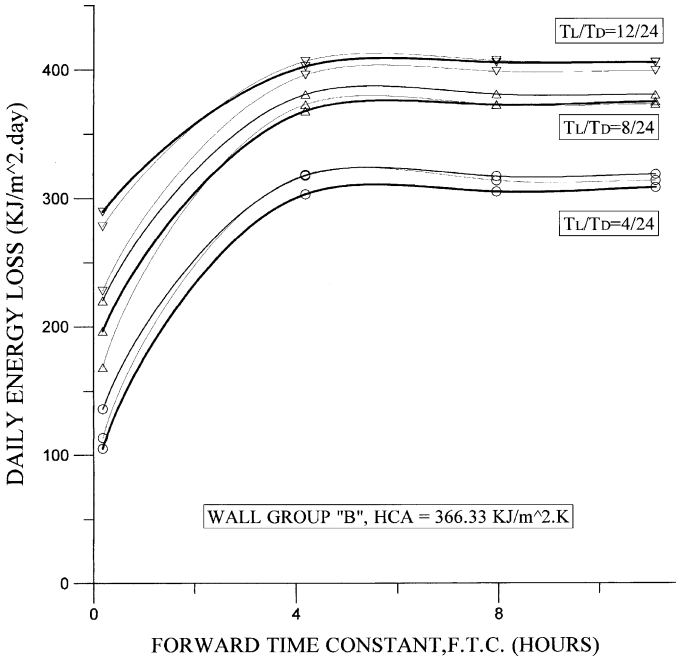

Fig. 6. The calculated quasi steady-state energy lost daily for the walls of the group B as a function of the forward wall time constant.

In each figure, the three plotted curve groups with the three curves each, correspond to a heating cycle of 4 h (T_L/T_D = 4/24), 8 h (T_L/T_D = 8/24) and 12 h (T_L/T_D = 12/24) daily, with a starting time t = 0, 6 and 12 h represented by thick, thin and very thin solid lines, respectively.

By comparative inspection between these figures it is derived as a general rule that the quasi steady-state energy losses from the intermittently heated space increases remarkably as the forward time constant increases from its initial very small value to about 3 h, while for further increase the losses are stabilized to a rather constant level. For the walls of the group A and a heating cycle duration of 4, 8 and 12 h daily, this level is in the order of 230, 160 and 120%, respectively, higher than the corresponding minimum time constant value. This increase is even more pronounced as the wall heat capacity increases to the level of the group B, with corresponding figures of about 270, 180 and 130% and group C of about 300, 190 and 140% for (T_L/T_D) = 4/24, 8/24 and 12/24, respectively. This suggests that for the intermittently heated buildings the thermal performance of walls with the thermal insulation layer placed at the room side is much higher and therefore should be preferred, as also previously noted by Kossecka and Kosny [11], especially for the short daily heating cycles.

As derived from the comparative inspection between Figs. 5–7, the effect of the heating cycle starting time on the wall daily energy loss is much more pronounced for walls of low forward time constant and heat capacity HCA, as can be seen in Fig. 5. As the per unit area heat capacity increases from 244.89 to 487.78 kJ/m^2 K, its effect tends to diminish, especially for the walls with higher time constant values as shown by Figs. 6 and 7. Inspection of the derived results leads to the general conclusion that the daily energy loss tend to increase as the starting time of heating cycle increases from t = 0 to 6 h. Further subsequent increase to 12 h however leads to a decrease of energy loss, except in the case of the longer 12 h heating cycle for the walls of group A. This is attributed to the combined effect of dynamic wall processes, causing a remarkable phase lag of the meteorological driving forces, which determine considerably the heat losses.

It is also derived that, although not proportionally, the energy loss increases with the time duration of the heating cycle, so as for walls of forward time constant higher than about 4 h, the effect of increasing the heating cycle duration by a factor of 2 and 3 leads to a respective increase of energy loss by a factor of only 1.2 and 1.35, almost irrespectively to the wall heat capacity HCA and starting time. However, for walls of much lower time constant, the same increase of the heating cycle duration leads to a considerably higher corresponding increase of energy loss, typically by a factor of 1.8 and 2.4, which also depends considerably stronger now on the starting time and wall heat capacity, HCA.

The parametric effects of the per unit floor area net power input q_n and (V/A_f) ratio on the daily energy loss are shown in Fig. 8, in which the daily energy loss is plotted against the forward time constant for the B group of walls, corresponding to HCA = 366.34 kJ/m^2 K. In this plot, three groups corresponding to (V/A_f) = 0.7m (lower group), 3 m (intermediate group) and 6 m (upper group) of two lines each were plotted. Both lines in each group, which correspond to q_n = 37 W/m^2 (lower line) and q_n = 75 W/m^2 (upper line), are very close together as happens with (V/A_f) = 7 m, while with those referring to the (V/A_f) = 3 m being almost indistinguishable and those to (V/A_f) = 0.7 m completely identical. As derived from the plotted results it can be seen that for a fixed (V/A_f), the effect

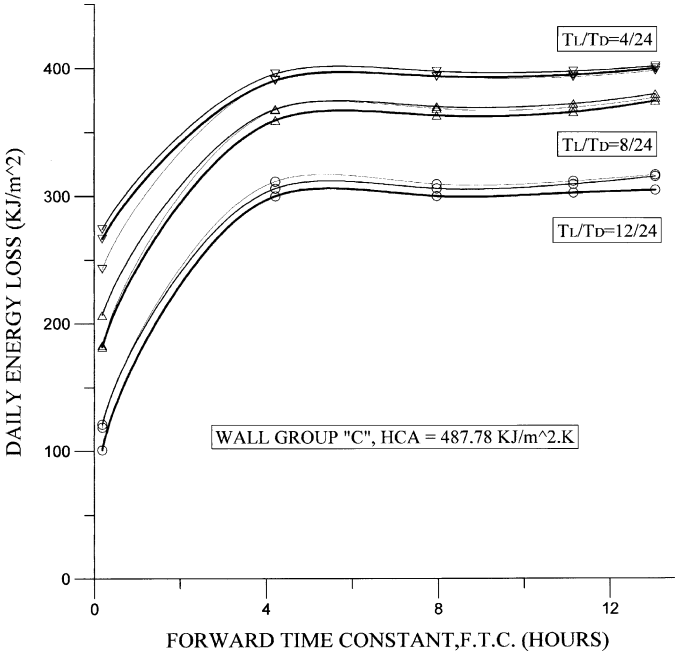

Fig. 7. The calculated quasi steady-state energy lost daily for the walls of the group C as a function of the forward wall time constant.

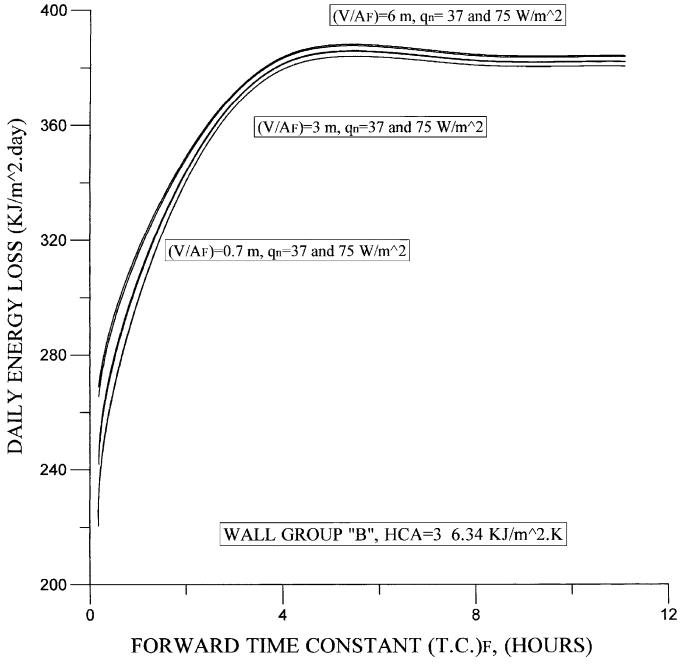

Fig. 8. Results from the sensitivity analyses showing the influence of the parametric values of q_n = 37 and 75 W/m^2 and (V/A_f) = 0.7, 3 and 6 m on the energy lost daily for the walls of the group B.

of varying q_n by a factor of 2 leads to a negligible difference between derived results, especially for $(V/A_f) = 0.7$ m. For walls of a low forward time constant of about 0.4 h the effect of almost an order of magnitude variation of the parameter (V/A_f) from 0.7 to 6 m leads to about 9% difference between results, while for forward time constants higher than about 4 h this difference decreases to about 1.2%.

6. Conclusions

An analysis was developed to investigate the effects of various thermal insulation configuration and heating system operational parameters on the quasi steady-state energy loss from structural elements of the building envelope like walls and roofs. The analysis was based on extensive simulation results on the transient thermal behavior of three different wall groups of uniform thermal resistance and heat capacity each, under the effect of intermittent heating and typical winter meteorological driving forces representative of a mild Mediterranean climate. It was derived that the increase of forward wall thermal time constant, which is caused by the distribution of a large heat capacity close to the room side, leads to the considerable increase of transient and decrease of quasi steady-state room node daily temperature swing owing to the associated effects of heat storage. The heating cycle duration leads to the reduction of transient duration and quasi steady-state room node daily temperature swing, which is weakly depended on the heating cycle starting time. A strong dependence was found between quasi steady-state daily energy loss and forward wall time constant, almost irrespective of all other parameters like wall heat capacity, heating cycle duration and starting time. Also the daily energy loss increases strongly as a function of forward time constant up to values corresponding to about 3 h, while for further increase of forward time constant they are rather stabilized to a more or less constant level. This confirms that for intermittently conditioned spaces, the thermal insulation perform better when installed at the interior wall side. The daily quasi steady-state energy losses are also proportional to the wall heat capacity for fixed values of forward time constant. The effect of the heating cycle starting time on wall daily energy loss is much more pronounced for walls of low forward time constant and heat capacity. For higher wall heat capacities the effect of starting time tends to diminish, especially for higher wall thermal time constants. The daily energy losses also increase with the time duration of the heating cycle, especially for the lower values of the forward time constant, and depend weakly on the wall heat capacity and heating cycle starting time.

Finally the derived results are almost insensitive to the effects of room node heat capacity and per unit area heat power input, respectively, at least as far as the investigated range of the corresponding parameters is concerned.

References

[1] J. Maloney, T.-C. Wang, C. Bing, J. Thorp, Thermal network predictions of the daily temperature fluctuations in a direct gain room, Solar Energy 29 (3) (1982) 207–223.
[2] R.J. Duffin, G. Knowles, A passive wall design to minimise building temperature swings, Solar Energy 33 (3/4) (1984) 337–342.
[3] F. Haghighat, T.E. Unny, M. Chandrashekar, Stochastic modelling of transient heat flow through walls, ASME Journal of Solar Energy Engineering 107 (1985) 202–207.
[4] A.K. Athienitis, H.F. Sullivan, K.G.T. Hollands, Analytical model, sensitivity analysis and algorithm for temperature swings in direct gain rooms, Solar Energy 36 (4) (1986) 303–312.
[5] P.T. Tsilingiris, On the transient themal behavior of structural walls—the combined effect of time-varying solar radiation and ambient temperature, Renewable Energy 27 (2002) 319–336.
[6] N.W. Wilson, W.G. Colborne, R. Ganesh, Determination of thermal parameters for an occupied house, ASHRAE Transactions 90 (Part 2B) (1984) 39–50.
[7] R.R. Crawford, J.E. Woods, A method for deriving a dynamic system model from actual building performance data, ASHRAE Transactions 91 (Part 2B) (1985) 1859–1874.
[8] J.E. Christian, J. Kosny, Thermal performance and wall ratings, ASHRAE Journal (March) (1996) 56–65.
[9] P.T. Tsilingiris, Thermal flywheel effects on the time varying conduction heat transfer through structural walls, Energy and Buildings 35 (2003) 1037–1047.
[10] P.T. Tsilingiris, On the thermal time constant of structural walls, Applied Thermal Engineering 24 (2004) 743–757.
[11] E. Kossecka, J. Kosny, Influence of insulation configuration on heating and cooling loads in a continuously used building, Energy and Buildings 34 (2002) 321–331.
[12] P.T. Tsilingiris, The influence of heat capacity and its spatial distribution on the transient wall thermal behavior under the effect of harmonically time-varying driving forces, Building and Environment 41 (2006) 590–601.
[13] Handbook of Heat Transfer, McGraw-Hill, New York, 1973.
[14] D.R. Croft, D.G. Lilley, Heat Transfer Calculations using Finite Difference Equations, Applied Science Publishers, London, 1977.
[15] J.A. Duffie, W.A. Beckmann, Solar Engineering of Thermal Processes, Wiley, New York, 1980.
[16] P.T. Tsilingiris, Solar water heating design—a new simplified dynamic approach, Solar Energy 57 (1) (1996) 19–28.
[17] P.T. Tsilingiris, Design, analysis and performance of low-cost plastic film large solar water heating systems, Solar Energy 60 (5) (1997) 245–256.
[18] Handbook ASHRAE, Fundamentals Volume, ASHRAE, Atlanta, GA, 1981.